

An Optimal Phase-Control Strategy for Damped-Driven Duffing Oscillators

Supplementary Material

R. Meucci,^{1,2,3} S. Euzzor,¹ E. Pugliese,^{1,4} S. Zambrano,⁵ M.R. Gallas,^{1,2,3} and J.A.C. Gallas^{1,2,3}

¹Istituto Nazionale di Ottica, Consiglio Nazionale delle Ricerche, Largo E. Fermi 6, Firenze, Italy

²Departamento de Física, Universidade Federal da Paraíba, 58051-970 João Pessoa, Brazil

³Instituto de Altos Estudos da Paraíba, Rua Infante Dom Henrique 100-1801, 58039-150 João Pessoa, Brazil

⁴Dipartimento di Scienze della Terra, Università degli Studi di Firenze, Via G. La Pira 4, Firenze, Italy

⁵Università Vita-Salute San Raffaele, Via Olgettina 58, 20132 Milano, Italy

(Dated: January 4, 2016 às 7:49)

I. EXPERIMENTAL SETUP

The experimental setup used in our experiments is illustrated in Fig. 1. Briefly, it consists of two integrators I_1 and I_3 whose outputs are the signals x and $y = \dot{x}$ contained in Eq. 1. The other two integrators, I_2 and I_4 , are employed for two inverting amplifiers with unitary gain. The cubic nonlinearity x^3 is realized by means of two analog multipliers M_1 and M_2 . The third one, M_3 , allows phase control to the double well oscillator.

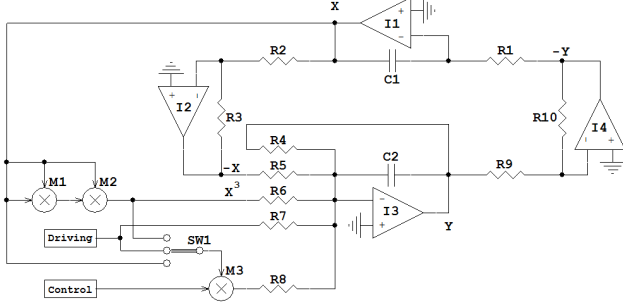


Figure 1. Duffing's oscillator circuit with phase control. I1 and I3 integrators (LT1114); I2 and I4 inverting amplifiers (LT1114); $C1 = C2 = 10 \text{ nF}$; $R1 = R2 = R3 = R5 = R6 = R7 = R9 = R10 = 10 \text{ k}\Omega$; $R4 = 40 \text{ k}\Omega$; $R8 = 110 \text{ k}\Omega$; $M1, M2$ and $M3$, multipliers (MLT04). SW1 is a 3 poles one track switch allowing the selection of phase control on the variable x, x^3 and driving. Driving and Control are sinusoidal function generators.

II. SINGLE WELL DUFFING OSCILLATOR

In this section, we would like to show the differences emerging when phase control is applied to the double well Duffing oscillator and the single well Duffing oscillator. In the former case the dynamics is described by the following differential equation:

$$\ddot{x} + b\dot{x} + f(t) \cdot x + x^3 = A \cos(\omega t), \quad (1)$$

$$\ddot{x} + b\dot{x} + x + f(t) \cdot x^3 = A \cos(\omega t), \quad (2)$$

where $f(t) = 1 + \varepsilon \cos(m\omega t + \varphi)$. In these equations, $m = 1$, the damping rate is $b = 0.25$, and A is the amplitude of the driving term.

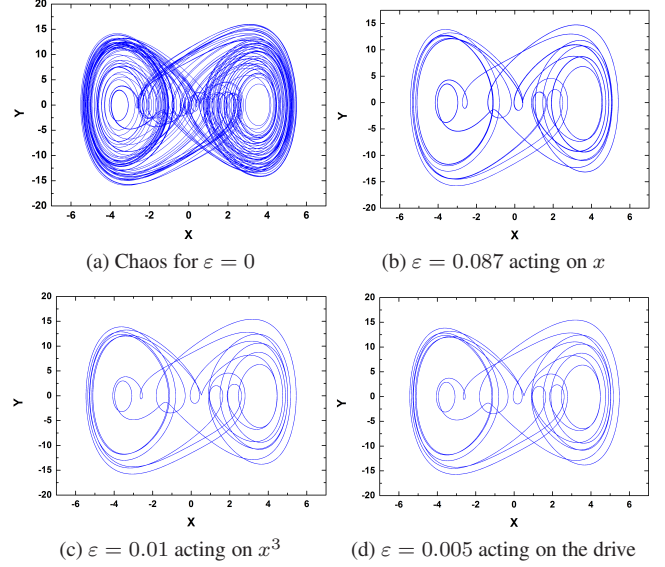


Figure 2. Representative attractors obtained for a *single-well* Duffing oscillator when $A = 51$. The following values of φ (indicated by points in Fig. 3) produce identical plots: $\varphi = 1.645$, and 4.88 for x , $\varphi = 0.199, 3.34$ and 6.135 for the x^3 , and $\varphi = 0.199, 3.34$ and 6.135 for the driving. For the case of perturbation on x^3 we verify that the periodic orbit (b) is also stabilized for $m = 3$ but not for $m = 2$, confirming the role of asymmetries in single-well Duffing.

It possesses a stable fixed point at the origin of the phase-space (x, \dot{x}) and can show chaotic behavior as the amplitude of the driving term is increased. In order to make a comparison with the double valley potential we assume . At $A = 51$ the dynamics is chaotic as reported in Fig. 2a. The initial conditions selected for the integration are $x_0 = 1.89$ and $y_0 = 0$.

If we apply phase control to this chaotic situation we see that it is possible to stabilize two nearly coinciding periodic orbits shown in Fig. 2b and Fig.2c. In the first case (2b), the stabilized orbit is obtained perturbing the linear term in the force term with an amplitude strength $\varepsilon = 0.087$, while in the second case (2c) the perturbation is $\varepsilon = 0.01$. This difference is related to the fact in this case the dynamics is confined in single potential valley and when it results chaotic is visiting phase-space with amplitudes greater than 1. As a consequence, a perturbation on the cubic term is more efficient to redirect a chaotic trajectory on a periodic attractor than a per-

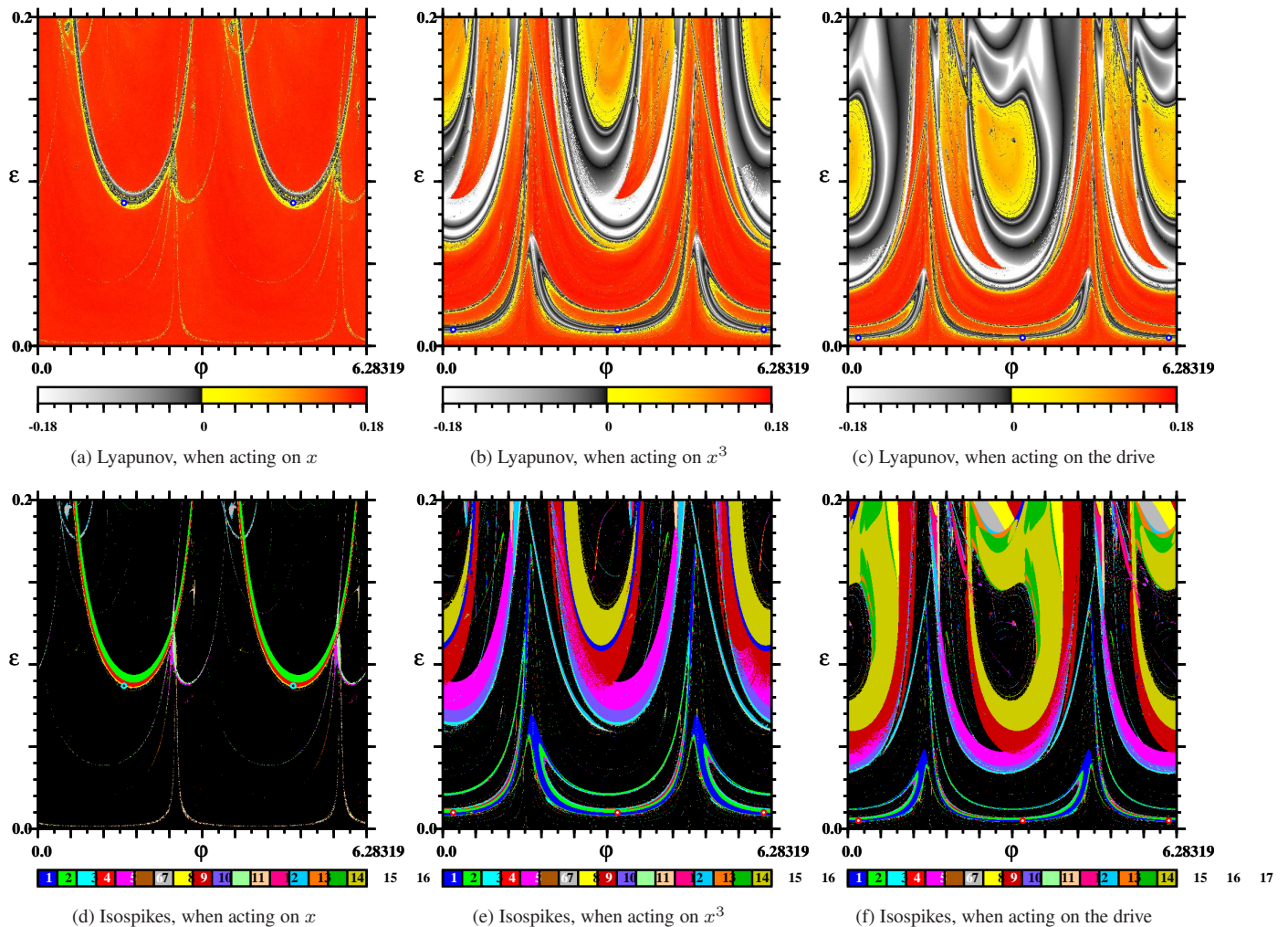


Figure 3. Stability charts for the *single-well* Duffing oscillator: Lyapunov exponents (top row) and isospike diagrams (bottom row). Here $A = 51$, $b = 0.25$, $m = 1$. Points (φ, ε) given in Fig. 2(b) are indicated, with colors chosen for maximal contrast. A total of $6 \times 600 \times 600 = 2.16 \times 10^6$, i.e. more than 2 million parameter points are displayed.

turbation on the linear term. The case of chaotic motion in a double potential well see the competing role of two stable fixed point located at $(-1, 0)$ and $(1, 0)$ and the unstable point at the origin $(0, 0)$. In such a case, the trajectory is confined between the two valleys and affected by the unstable node at the origin. As a consequence, a perturbation applied to the linear term is comparable with that on the cubic term.

III. THE REAL-TIME INDICATOR

Our real time indicator allows a separation between chaos and periodicity (regularity).

The indicator is based on low pass filter and a discriminator with adjustable threshold. In our case the input signal of the low pass filter is the signal $z = x^2 + y^2$ which will positive definite. The operation of low pass filter implies a first-order

differential equation for the output signal v :

$$\dot{v} = -(v - z)/\tau, \quad (3)$$

where τ is the time constant of the filter. If the input filter z is a periodic function, the output signal v will oscillate around its mean value with small periodic fluctuations. In the chaotic case, the output signal will oscillate around a lower mean value with large fluctuations due to its higher content of harmonics. In this way, if a given threshold is selected on the discriminator we are able to distinguish the two regimes. When the dynamics is chaotic the output signal of the indicator will oscillate between two levels (0 and 1). On the contrary, when the solutions are periodic, the filtered signal converges to its average value with small residual periodic oscillations and is easily discriminated.